Nanoscale

Dynamic Article Links ►

Cite this: DOI: 10.1039/c0xx00000x

www.rsc.org/xxxxxx

ARTICLE TYPE

SERS substrate for detection of explosives

Alison Chou,*[a] Esa Jaatinen,[a] Ricardas Buividas,[b] Gediminas Seniutinas,[b] Saulius Juodkazis,[b,c] Emad L. Izake,[a] Peter M. Fredericks[a]

Received (in XXX, XXX) Xth XXXXXXXXX 20XX, Accepted Xth XXXXXXXXX 20XX

DOI: 10.1039/b000000x

A novel gold coated femtosecond laser nanostructured sapphire surface – an "optical nose" - based on surface-enhanced Raman spectroscopy (SERS) for detecting vapours of explosive substances was investigated. Four different nitroaromatic vapours at room temperature were tested. Sensor responses were unambiguous and showed response in the range of 0.05 – 15 μM at 25 °C. The laser fabricated substrate nanostructures produced up to an eight-fold increase in Raman signal over that observed on the unstructured portions of the substrate. This work demonstrates a simple sensing system that is compatible with commercial manufacturing practices to detect taggants in explosives which can undertake as part of an integrated security or investigative mission.

1. Introduction

Creation of an optical detection system – the "optical nose" – for efficient recognition and discrimination between explosives, volatile organic compounds (VOC), and toxic gases is an area of intense research activity, that is of significant interest to agencies responsible for security, law enforcement, air quality and environmental monitoring.[1] To be practical, this technology must offer rapid response, ultrasensitivity and the capability for remote substance detection. Although the limit of detection (LOD) requirement for a gas sensor depends on the particular application, sensitivity in the parts per billion level (with 1 ppb considered the canine limit of detection benchmark) is considered acceptable and the minimum required for the detection of VOCs in modern green buildings for air quality monitoring.

Currently, the presence of explosive vapours and chemical warfare agents can be measured with quartz crystal microbalances,[2] gas chromatography,[3] capillary electrophoresis,[4] and ion mobility spectroscopy.[5] These methods, however, are laboratory based, not instantaneous, and require specific sample preparation. Lack of specificity and sensitivity are also limiting issues with these instrumentation complex techniques; and the signals obtained cannot distinguish between different components of the analyte.

Though Raman scattering has been used as a powerful "chemical fingerprint" technique for almost 80 years, it is a weak scattering process and in general perceived to be not practical for trace gas determination. Detection sensitivity can be increased by using nanostructured metallic surfaces to enhance the Raman signal by many orders of magnitude [6] making the detection of single molecules possible.[7] While surface enhanced Raman scattering (SERS) has considerable potential, the difficulty in fabricating reproducible SERS substrates that give reproducible signal response with high sensitivity for the particular application is proving a significant challenge that is limiting the development of a SERS based gas detection device.

Here we present a novel gold coated femtosecond laser nanostructured sapphire surface as an optical nose for detecting vapours of explosive substances when interrogated using Raman spectroscopy. The sensing substrate comprises a laser structured sapphire wafer α–Al_2O_3 (001) coated with a 10 nm thick gold film by plasma sputtering. Laser nanostructuring using femtosecond laser pulses is a practical alternative to lithography-based multi-step techniques and is widely used in micro-optical applications.[8] Nano-texturing of surfaces by laser ablation show promise for light extraction applications with light emitting diodes (LEDs) and can be used for micro-optical elements on the surface or inside the substrates of LEDs. In dielectrics, ablation by ultra-short (sub-picosecond) laser pulse creates self-organized relief structures, ripples, which can have periods 100-200 nm even with a laser writing wavelength of ~1 μm.[9] It was recently shown that in comparison to commercial lithographically fabricated substrates, the sensitivity of the gold coated ripples fabricated on sapphire surpasses the commercial substrate by a factor of more than 10 with a spot-to-spot reproducibility that is a factor of 2 better.[10]

The detection mechanism takes place on the sensor surface where light is incident directly on the optical nose chip where the vapour molecules are adsorbed. The inelastically scattered photons from the vapour molecules are detected by a CCD camera. The optical nose fabricated by laser nanostructuring shows great promise as a viable technique for fabricating sensitive and reusable vapour sensors. As we show in this work, light field enhancement on metallic nano-sized features can exceed a factor of 30. Furthermore, the nanostructures on the

surface of the sensor increases sensitivity and lower the detection limit due to the high surface-to-volume ratio. The deposition of gold on the sapphire allows the nitro moiety, present in many high explosives,[11] to adsorb onto the substrate through its oxygen atoms to form a bidentate surface chelate[12] thus immobilizing analytes of interest for detection. To reuse the sapphire substrate, the gold film is dissolved in a solution of aqua regia and recoated with fresh gold without any degradation of sensitivity.

The capability of the structured sapphire substrate as a sensing platform for nitroaromatic vapours is demonstrated by 2,4-dinitrotoluene (2,4-DNT), 2,4-dinitrochlorobenzene (2,4-DNCB), *p*-nitroaniline and nitrobenzene as model compounds. All compounds consist of a benzene ring with at least one nitro functional group. 2,4-DNT is commonly used for testing Raman scattering explosive sensing devices.[13] However, literature results on 2,4-DNCB and *p*-nitroaniline vapour detection using Raman spectroscopy are more rare. We have specifically included 2,4-DNCB in our test because its vapour pressures at ambient temperature are lower than the commonly tested 2,4-DNT. The equilibrium vapour concentration at ambient temperature for these compounds range between 0.2 µM for *p*-nitroaniline to 15 µM for nitrobenzene (Table 1). This range of concentration is difficult to detect with conventional Raman spectroscopy.

Here we demonstrate that the nano-structured sapphire substrate can enhance the Raman signal of the selected test compounds to detect the vapours at room temperature, and hence explore the feasibility of using the substrate and Raman spectroscopy for practical detection of explosive vapours. Another complementary aim is concerned with the mechanism behind the Raman signal enhancement. We show numerically and confirm experimentally that some of the observed enhancement results from increased surface reflectivity and depends on the gold film thicknesses. Experimental and simulation results are in good agreement.

Table 1. Vapour pressure of test compounds

Test compound	Vapour pressure at 25 °C/mmHg	Equilibrium vapour concentration at 25 °C (µM)	Equilibrium vapour concentration at 25 °C (ppm)
2,4- DNCB	0.001[a]	0.05	11
2,4-DNT	0.002[a]	0.11	20
p-NA	0.004[b]	0.20	28
Nitrobenzene	0.270[a]	15.0	1813

[a] Royal chemical Society chemical structure data base [b] Sigma–Aldrich Australia

2. Results and discussion

Figure 1a shows the SEM image of the structured and unstructured regions of the sapphire surface. In contrast to the featureless unstructured sapphire surface, the femtosecond laser induced modification of the sapphire shows ablation "ripple" patterns characterised by grooves and a layered pattern with a layer thickness of around 240 nm. Figure 1b and 1c show the 2,4-DNT signals from the nano- structured and the unstructured gold coated sapphire substrates, after exposing the substrates to 2,4-DNT vapour for 18 h at 25 °C. It is notable that the spectrum from the structured portions of substrate shows a marked increase in intensity and more bands than the spectrum obtained from the unstructured portions of the sapphire surface. The spectrum from the structured substrate shows three main Raman bands at 1355 (NO_2 symmetric stretch), 837 (NO_2 scissors mode) and 793 cm^{-1} (C-N stretch mode). On the other hand, the unstructured substrate shows only one band at 1353 cm^{-1} and of insufficient intensity to merit identification as 2,4-DNT. As a substrate for sensing applications, such a weak, single Raman band means the compound cannot be identified with confidence. This result shows that the structuring of the sapphire surface is critical in increasing the Raman signal strength thus improving the sensitivity of the sensor.

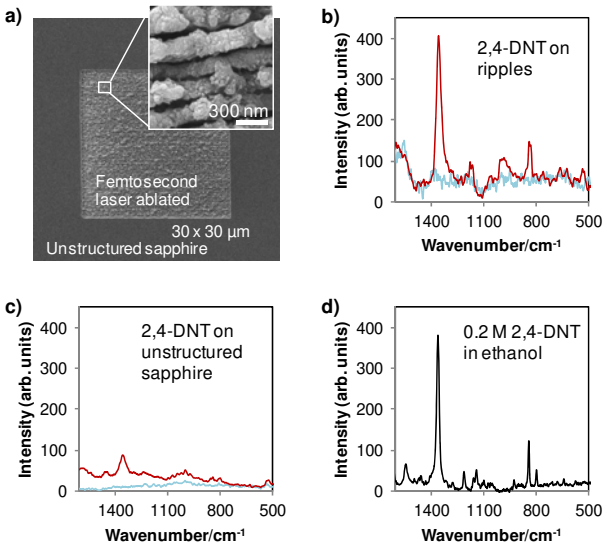

Figure 1. a) SEM images showing the surface morphology of a 30 x 30 µm area fabricated using a Ti:Sapphire femtosecond pulse laser operating at central wavelength of 800nm with pulse duration of 150 fs. b) Raman spectra of the gold coated ripple substrate and c) gold coated unstructured sapphire before (blue) and after exposure (red) to 2,4-DNT vapour at 25 °C. d) Normal Raman spectrum of 0.2 M 2,4-DNT in ethanol after subtracting the spectrum of pure ethanol.

Figure 2 shows the results obtained from the structured substrate from the other three nitroaromatic compounds tested. The overlaid reference spectra have been rescaled for comparison purposes. From the spectra, the presence of the nitro group of the compound can be inferred; all four compounds tested show a prominent key spectral -NO_2 symmetric stretch at ~1350 cm^{-1}. It is important to note that a complete match of the spectra is not expected. This is because the presence or absence of modes is related to the orientation of the molecule at the surface and also due to change in polarizability of the molecule upon adsorption to the gold surface.[14,15] When molecules are adsorbed onto a metal surface, the symmetry and the field gradient of Raman scattering also change. In the case of adsorption, vibrational modes associated with the analyte moiety closest to the surface will be the most enhanced.[14,16] The complete experimental Raman frequencies for the observed vibrational modes with corresponding assignments presented in Table 2. Bands were

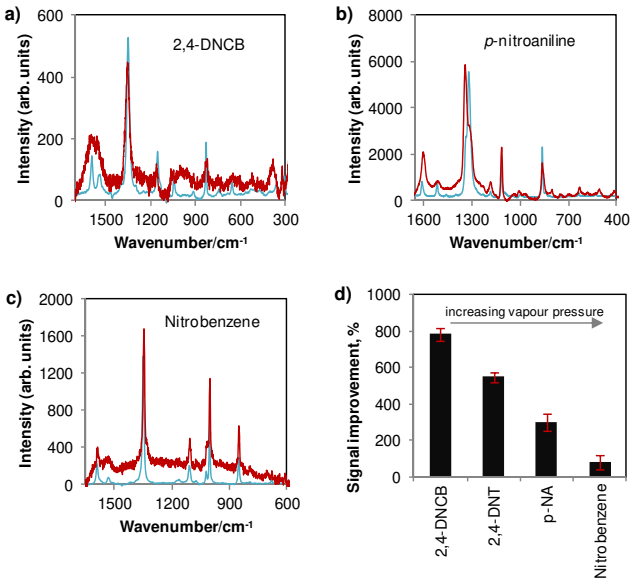

Figure 2. Raman spectra of vapour detection at the 10 nm gold coated structured sapphire substrate (red spectra) compared with the reference (blue spectra). a) 2,4-DNCB, b) *p*-nitroaniline, and c) nitrobenzene. Reference spectra correspond to analyte dissolved in ethanol, after subtracting the ethanol spectrum. d) Signal improvement of structured over unstructured sapphire substrate based on the integrated peak intensity of the $-NO_2$ symmetric vibration band near 1348 cm^{-1}.10 randomly selected areas across each substrate were sampled.

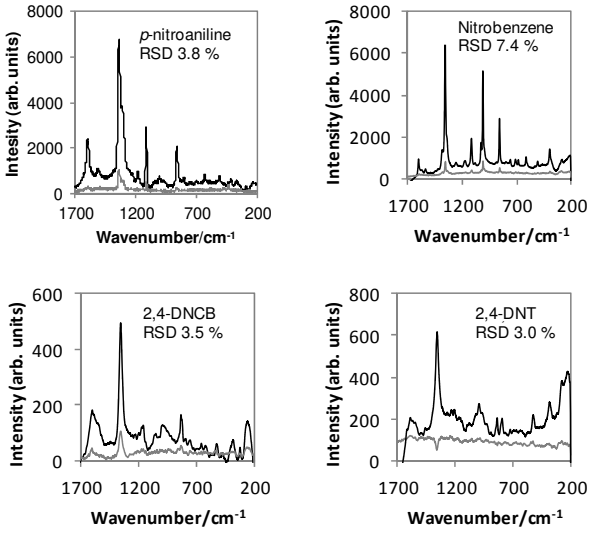

Figure 3. Reproducibility of sensor signal. Averaged Raman spectra of *p*-nitroaniline, nitrobenzene, 2,4-DCNB and 2,4-DNT from mapping data sets. The average spectrum was calculated from 10 spectra recorded from different areas of the ripple substrate. The average spectrum is shown in black. Grey spectrum corresponds to the standard deviation of the 10 spectra.

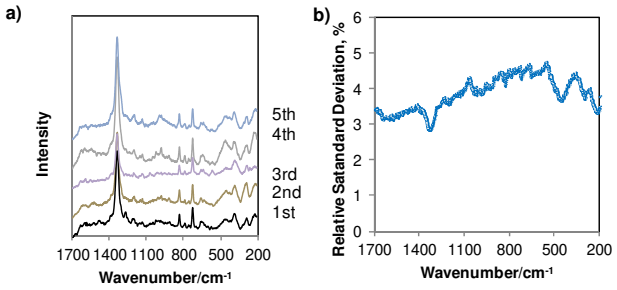

Figure 4. Assessment of repeated usage of a given ripple substrate. a) Raman spectra of 2,4-DNT vapour detected at room temperature on the ripple substrate. The ripple substrate was subjected to 5 cycles of rinsing in aqua regia and gold coating between each use. b) Relative standard deviation of signal intensity as a funciton of wavenumber.

assigned according to previous studies carried out on 2,4-DNT,[13] nitrobenzene,[17] and *p*-nitroaniline[18] adsorbed on gold surfaces. It is interesting to note that the increase in signal intensity from the unstructured to modified substrate appears to be compound or vapour pressure dependent. Based on the integrated peak intensity of the $-NO_2$ peak near 1350 cm^{-1}, signals from the modified substrate are more intense by about 550% (Figure 2d). Of the four compounds tested, 2,4-DNCB shows the greatest difference; nearly an 800% increase, while nitrobenzene with a vapour pressure of 270 times higher than 2,4- DNCB at 25 °C only showed an 80% increase with the modified substrate. The reason why the enhancement is not consistent for different nitro compounds could be due to their assembly/orientation on the gold surface.

Another important factor evaluated for routine sensing application of the optical nose being investigated was the reproducibility of the sensor. Spot-to-spot reproducibility of the signal from the ripple substrate was assessed by Raman mapping wherein spectra were obtained from randomly selected areas. By comparing the spectral features within the mapping data sets, it can be seen in Figure 3 that the ripple substrate gives reproducible sensor performance with average standard deviation being below 8%. Figure 4 shows the reusability of the ripple substrate. Substrate reusability was assessed by removing the used gold coating with aqua regia, laying down a fresh gold coating and re-expose the substrate to 2,4-DNT at room temperature. All spectra in Figure 4a show clear fingerprint of 2,4-DNT Raman spectrum with good signal-to-noise-ratio. The average relative standard deviation of the Raman signal for the 5 repeated usage was ~3.8% (Figure 4b).

Raman signals from analytes attached to metallic surfaces have been shown to increase as the reflectivity of the surface increases.[19] Thus, one possible explanation for the variation in Raman signal strength between the structured and unstructured portions of the substrate is differences in the reflectivity of the gold film. The light field that produces the Raman signal is a combination of the incident light and that reflected from the gold film. The presence of a conducting surface can vary the laser intensity experienced by the molecule at the surface over a range from zero to four times the incident laser intensity.[14] Therefore, any increase in the amount reflected from the structured portion over that reflected from the unstructured portion could potentially explain the difference in Raman signal. Here we model the

amplitude and phase of the electromagnetic field at the gold surface and its influence on the Raman scattering. In our system, the electromagnetic field interacting with the analyte adsorbed on the gold is the sum of the incident field, the field reflected from the gold-air interface, and the field reflected from the gold-sapphire interface. In this instance the reflected intensity is added to the incident intensity due to the loss of coherence resulting from the locally rough gold surface formed during deposition.[20] For this three layered system, the transfer matrix method was used to determine the intensity reflection coefficient from the air-gold-sapphire slab which is:[20]

$$R = \frac{I_{\mathrm{ref}}}{I_{\mathrm{Inc}}} = \frac{r_1 + r_2 Exp[i2k'L]}{1 + r_1 r_2 Exp[i2k'L]} \frac{r_1^* + r_2^* Exp[-i2k'L]}{1 + r_1^* r_2^* Exp[-i2k'L]} \qquad (1)$$

here I_{inc} is the incident laser field amplitude, r_1 is the Fresnel field amplitude reflection coefficient of the light field from an air-gold interface (r_1^* is the complex conjugate of r_1), r_2 is the Fresnel field amplitude reflection coefficient for a gold-sapphire interface, k' is the wave-vector in the gold medium and L is the thickness of the gold film. The intensity of total field that interacts with the analyte is then simply the addition of the reflected intensity given by Eq. (1) and the incident field. Substituting in refractive index data for gold[21] and for sapphire into Eq. (1) reveals that for gold film thicknesses 70 nm or greater, the field intensity interacting with the analyte at the surface is approximately 1.8 times greater than the incident laser field at 785 nm alone. In addition, the reflective gold film also produces an additional enhancement of the Raman signal by reflecting the inelastically scattered Raman photons back towards the detector. Therefore the total Raman signal enhancement due to reflective effects can be expressed as:

$$\frac{Sig_{ref}}{Sig_{inc}} = (1 + R)^2 \qquad (2)$$

Here we assume that the wavelength dependent Fresnel field amplitude reflection coefficients, r_1 and r_2, are approximately the same for the elastically and inelastically scattered photons. Substituting refractive index data for gold and sapphire into Eq. (2), shows that the Raman signal enhancement increases to approximately 4 for a gold film thickness of around 70 nm or more for an excitation wavelength of 785 nm. This was verified by varying the gold coating thickness on the sapphire substrate. The Raman signal intensity increased with increasing gold coating thickness from 10 to 70 nm for nitrobenzene (Figure 5a, c) and from 10 to 100 nm for 2,4-DNT (Figure. 5b, c). This observed dependence of Raman signal on gold film thickness agrees well with the theoretical prediction as shown in Figure 3d. Importantly the Raman signal intensity observed from both the structured and unstructured portions of the substrate displayed the same trend – an increase in signal by approximately the same factor as the film thickness increased from 10 nm. This means that the increase in the observed Raman signal from the structured portion over the unstructured portion of the substrate, as shown in Figures 1 and 2, is not the result of increased film reflectivity. In fact, due to the increased roughness of the structured surface its reflectivity is actually lower than that of the unstructured portion[20]. Therefore, it can be concluded that the laser induced nanostructure itself is responsible for the signal enhancement shown in Figure 3. With the structured surface, the most intense Raman signal was obtained at 75 nm and 140 nm for nitrobenzene and 2,4-DNT respectively. Beyond these maxima, the Raman signal decreases with further increase in film thickness. Studies on film thickness and Raman intensity have been carried out by Schegel et al[22] and Zhang et al.[23] Both studies consistently showed a steady increase in signal for increasing metal film thickness until a maximum Raman signal is reached followed by a decrease for any further increase in film thickness. A commonly accepted explanation for this observed trend is the modulation of the surface plasmon absorption by the thickness of the metal film. As the gold film thickness increases, it forms a continuous structure therefore becoming a poor SERS enhancer.[23]

Table 2. Observed Raman frequencies of 2,3-DNT, 2,4-DNCB, *p*-nitroaniline and nitrobenzene

Test compound	Raman frequency in wavenumber units (cm^{-1})		Assignment [c]
	Adsorbed on gold	In ethanol solution	
2,4-DNT		1616	C=C aromatic str.
		1540	C-C str
	1355	1356	NO_2 sym. str.
		1207	C-H
	837	835	NO_2 scissors mode
	793	793	C-N str.
2,4-DNCB	1592	1597	C-C str.
	1354	1357	NO_2 bending
p-nitroaniline		1455	CC str.
	1599	1606	CC str.
	1510	1513	NO_2 asym. Str.
	1338	1334 (shoulder)	NO_2 asym. Str.
	1312 (shoulder)	1318	C-NO_2 str.
	1182	1181	CH-plane bend
	1112	1114	CH in-plane bend
	861	862	NO_2 bend
	628	633	ring def.
Nitrobenzene	508		NO_2 rock
	1592	1592	C-C str.
	1349	1352	NO_2 sym.
	1004	1004	Trigonal ring def.
	853	853	NO_2 bending

[c] Abbreviations: str, stretching; def, deformation vibration; sym, symmetric; asym, asymmetric. Assignments are based on studies in references 12, 16 and 17.

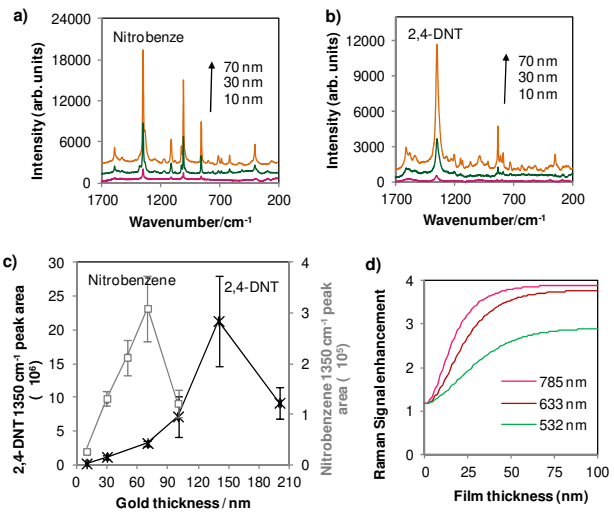

Figure 5. a) Nitrobenzene and b) 2,4-DNT signal from structured sapphire substrate with different gold coating thickness. c) Raman peak intensities of the NO_2 symmetric stretching mode (near 1334 cm^{-1}) as a function of gold coating thickness for nitrobenzene and 2,4-DNT. d) Theoretical Raman signal enhancement due to increased reflectivity of underlying film as predicted by Eq. (2).

We note also that while the spectral features of nitrobenzene did not vary significantly with layer thickness, the 2,4-DNT spectra show a remarkable difference with a thicker layer of gold. Not only do the bands appear more intense, but the bands that were absent with the 10 nm coating could be seen with the thicker coating, suggesting that a thicker layer of coating could increase the sensitivity of the substrate. This is important as there is a great need for improved sensitivity and reliability of explosives Raman based sensors. This result shows that the sensor performance can be optimized with a gold coating of 70 nm or thicker.

Raman signal intensity markedly depends on the structure of the sapphire surface and the gold coating thickness on the substrate surface as illustrated through the structured and unstructured sapphire substrate used here. The spectra show significant differences in both intensity and number of bands. These differences signify the strong influence of the nanostructures on the substrate surface and that the use of the structured substrate leads to a substantial surface enhancement effect which was of the order of 10 when compared to the signal obtained from the unstructured gold.

The strength of Raman signal intensity further increases as the gold coating thickness increases, to a maximum at ca. 70 nm. It might therefore be expected that an improvement in the sensitivity of the sensor could be achieved when nanostructured surfaces are used as a substrate for detecting low vapour pressure analytes using Raman spectroscopy. Since many explosives include a nitro or nitroaromatic group, our work demonstrates the potential application of the substrate for detecting nitro-based explosives. The limit of detection of the sensor, estimated from the lowest ambient vapour pressure compound tested; 2,4-DNCB, was approximately 1 ppm based on the surface enhancement effect by a factor of 10 observed with the ripple substrate. Further improvements of the sensitivity to the required 10-100 ppb level via time and area integration of detected signal are currently under exploration.

3. Conclusion

We have proposed and validated one mechanism by which Raman signal is enhanced on reflective metals substrate surfaces through comparison with numerical results and experimental data. An increase in the Raman intensity from molecules adsorbed on the gold coating on top of the sapphire substrate of a factor of 4 can be predicted from the incident and the reflected electromagnetic field. A further increase by a factor of up to 8 is possible by nanostructuring the sapphire substrate with a femto-second laser.

4. Experimental

Sapphire substrate preparation: Ripples on sapphire substrate, α–Al_2O_3 (001), were fabricated using a Ti:Sapphire femtosecond pulse laser Spitfire (Spectra Physics Inc.) operating at a central wavelength of 800 nm with a pulse duration of 150 fs. A high numerical aperture (NA = 0.7) objective lens (Mitutoyo Ltd.) was used to focus the laser pulses onto the polished surface of a 400μm thickness high purity LED-grade α–Al_2O_3 wafer in the (001) orientation. Different 30 μm x 30 μm areas of periodic ripples with periods ca. 240 nm were fabricated using linearly and circularly polarised laser beam. During fabrication the sample was mounted on high precision linear stages (Aerotech Inc.) and moved at a speed of 10 μm/s, the distance between parallel lines was fixed at 0.7 μm to ensure a 10-30% overlap between them. After fabrication, the samples were rinsed in acetone, ethanol and high purity water using an ultrasonic bath for 2 min in each solution. The period of ripples, Λ, is defined by the laser wavelength, λ = 800 nm, and refractive index of α–Al_2O_3 (001) at the laser writing wavelength, n = 1.7, as Λ = λ/(2n) [15]. Samples were characterized by scanning electron microscopy (SEM). The unstructured portions of the α–Al_2O_3 (001) substrate were used as controls.

Gold coating: Prior to use, the substrates were coated with 10 nm of gold. All gold coatings were prepared from 99.999% gold deposited onto the α–Al_2O_3 (001) substrates using a Leica EM SCD005 sputter coater, under argon. The pressure was 0.05 mbar and the working distance was 50 mm. The thickness of the gold film was varied by adjusting the sputtering time according to the data provided by the instrument manufacturer. To reuse the sapphire substrate for studying the impact of different gold coating thicknesses, the used substrates were dipped briefly in aqua regia to dissolve the gold.

Chemicals: Substrates were tested with nitrobenzene, *p*-nitroaniline, 2,4-dinitrochlorobenzene (2,4-DNCB) and 2,4-dinitrotoluene (2,4-DNT). All chemicals were purchased from Sigma-Aldrich and were used as received.

Substrate exposure to vapour: Substrates were exposed to vapours of the selected compounds by placing the substrate inside a 15 mL scintillation vial containing 1.0 mg of the test compound in an aluminium pan at 25°C. The exposure time was 1 min for

nitrobenzene and for 18 h for *p*-nitroaniline, 2,4-DNT and 2,4-DNCB before collecting the Raman spectrum. The longer exposure time was allowed due to the much lower vapour pressure of these compounds at 25 °C (see Table 1). At the end of the exposure period, samples were removed from the vials and analyzed with a Raman spectrometer.

Raman data collection: Raman spectra were recorded at 25 °C using a Renishaw inVia Raman microscope with a laser source emitting at 785 nm, and a 50× objective (Leica) lens. Each spectrum was collected as a single scan with 10 s exposure time. Measurements of the vapour on the substrates were obtained with a laser power of 20 mW at the sample by focusing the laser beam on the substrate surface after exposing the substrates to analyte vapour. Neat materials in ethanol solution for spectral reference purposes were obtained with 200 mW laser power. The concentration for each of the reference solutions was set at the solubility limit for each compound. Given the weakness of Raman scattering, the most concentrated possible solution is desirable for improving the signal to noise ratio. The concentrations of the reference solutions were 1.0, 0.2, 0.5, 0.2 M for nitrobenzene, *p*-nitroaniline, 2,4-DNCB and 2,4-DNT respectively. Reference spectra were obtained by subtracting the spectrum of pure ethanol from the solution spectra using GRAMS software.

Acknowledgements

A.C. would like to acknowledge the Australian Research Council for their support through the Linkage Project LP0882614: A new nano-sensor technology for the detection and identification of residual vapours explosives, drugs and chemicals in the air, QUT Analytical Electron Microscopy Facility, Dr. Llew Rintoul for insightful discussions on Raman spectroscopy.

Notes and references

[a] *School of Chemistry, Physics and Mechanical Engineering Faculty of Science and Engineering*
Queensland University of Technology
Brisbane 4001, QLD, Australia
E-mail: alison.chou@qut.edu.au
[b] *Centre for Micro-Photonics, Faculty of Engineering and Industrial Sciences*
Swinburne University of Technology
Hawthorn, VIC, 3122, Australia
[c] *Melbourne Centre for Nanofabrication, 151 Wellington Road, Clayton VIC 3168, Australia*

References

1 a) M. I. Stockman, *Phy. Today* **2011**, *64*, 39. b) N. A. Rakow, K. S. Suslick, *Nature* **2000**, *406*, 710.
2 G. Bunte, J.Hurttlen, H. Pontius, K. Hartlieb, H.Krause, *Anal. Chim. Acta*. **2007**, *591*, 49.
3 R. Batlle, H.Carlsson, P.Tollback, A. Colmsjo, C.Crescenzi, *Anal. Chem*. **2003**, 75, 3137.
4 T, Kishi, J. Nakamura, H. Arai, *Electrophoresis* **1998**, *19*, 3.
5 D. D. Fetterolf, T. D. Clark, *J. Forensic Sci.* **1993**, *38*, 28.
6 a) M. Fleischmann, P. J. Hendra, A. J. McQuillan, Chem. Phys. Lett. 1974, 26, 163; b) D. L. Jeanmaire, R. P. Van Duyne, J. Electroanal. Chem. 1977, 84, 1; c) M. G. Albrecht, J. A. Am. Chem. Soc. 1977, 99, 5215; d) J. A. Creighton , C. G. Blatchford, M. G. Albrecht, *J. Chem. Soc. Faraday Trans. 2*, **1979**,*75*, 790-798.
7 K. Kneipp, Y. Wang, H. Kneipp, L. T. Perelman, I. Itzkan, R. Dasari, M. S. Feld, *Phys. Rev. Lett*. **1997**, *78*, 1667.
8 a) R. R. Gattass, E. Mazur, *Nat. Photonics* **2008**, *2*, 219; b) L. Kuna, A. Haase, C. Sommer, E. Zinterl, J. R. Krenn, F. P. Wenzl, P. Pachler, P. Hartmann, S. Tasch, G. J. Leising, *Appl. Phys*. **2008**, *104*. 074507; c) E. K. Illy, M. Knowles, E. Gu, M. D. Dawson, *Appl. Surf. Sci*. **2005**, *249*, 354.
9 R. Buividas, L. Rosa, R. Sliupas, T. Kudrius, G. Slekys, V. Datsyuk, S. Juodkazis, *Nanotechnology* **2011**, *22*. 055304.
10. R. Buividas, P. R. Stoddart, S. Juodkazis, Ann. Phys. (Berlin), 2012, doi: 10.1003/andp.201200140
11 T. Urbanski, S. K. Vasudeva, *J. Sci. Ind. Res. India* **1981**, *40*, 51.
12 M. E. Bartram, B. E. Koel, *Surf. Sci*. **1989**, *213*, 137.
13 a) J. M. Sylvia, J. A. Janni, J. D. Klein, K. M. Spencer, *Anal. Chem*. **2000**, *72*, 5834; b) M. K. K. Oo, , C. F. Chang, Y. Sun, X. Fan, *Analyst* **2011**, *136*, 2811; c) J. Wang, L. L. Yang, S. Boriskina, B.Yan, B. M. Reinhard, Anal. Chem. **2011**, *83*, 2243.
14 A. Campion, Annu. Rev. of Phys. Chem. **1985**, *36*, 549.
15 H. Metiu, Progress in *Surf. Sci*. **1984**, *17*, 153.
16 J. A. Creighton, *Surf. Sci*. **1983**, *124*, 209.
17 P. Gao, M. J. Weaver, *J. Phys. Chem*. **1989**, *93*, 6205.
18 T. Tanaka, A. Nakajima, A. Watanabe, T. Ohno, Y. Ozaki, *J. Mol. Struct*. **2003**, *661*, 437.
19. Q. Zhou, Y. J. Liu, Y. P. He, Z. J. Zhang, Y. P. Zhao, *Appl. Phys. Lett.* **2010**, *97*, 121902.
20. C. L. Mitsas, D. I. Siapkas, *Appl. Optics* **1995**, *34*, 1678.
21 P. B. Johnson, R. W. Christy, *Phys. Rev. B* **1972**, 6, 4370.
22 V. L. Schlegel, T. M. Cotton, *Anal. Chem*. **1991**, *63*, 241.
23 Z. J. Zhang, T. Imae, *J. Colloid Interf. Sci*. **2001**, *233*, 99.